



ELSEVIER

Journal of Volcanology and Geothermal Research 106 (2001) 285–300

Journal of volcanology
and geothermal research

www.elsevier.nl/locate/jvolgeores

Melt segregation by localized shear deformation and fracturing during crystallization of magma in shallow intrusions of the Otoge volcanic complex, central Japan

N. Geshi

Department of Earth and Planetary Science, Graduate School of Science, The University of Tokyo, 7-3-1 Hongo, Bunkyo-Ku, Tokyo 113-0033, Japan

Received 9 February 2000; accepted 20 October 2000

Abstract

Basaltic dikes and sheets in the Miocene Otoge volcanic complex in central Japan have thin trachyte veins, which exhibit systematic variation regarding spacing with distance from the dike wall. Compositional relationship between the trachyte veins and surrounding basalt shows that the trachytic melt filling the veins was formed by in situ fractionation and segregated from the surrounding basalt. Mass balance calculation suggests that a residual liquid of trachyte composition formed when about two-thirds of the parent basaltic magma was crystallized. Preferred orientation of groundmass crystals around the trachyte veins and echelon alignment of veinlets show that localized shear caused the deformation and fracturing in the incompletely crystallized magma and the interstitial residual melt was drawn into the fractures to form trachyte veins. The parallel development of trachyte veins and the increase of spacing toward the inner portion of the dike were controlled by the balance of cooling from the dike wall and segregation of interstitial melt. In a mobile magma body, shear will be concentrated in a crystal-mush layer in marginal parts, and the shear deformation could be an important mechanism to separate strongly-evolved residual melt from a mushy crystallizing layer. © 2001 Elsevier Science B.V. All rights reserved.

Keywords: trachyte vein; melt segregation; fracturing; shear dilatancy; Otoge volcanic complex

1. Introduction

Separation of residual melt from mixtures of crystals and melt is a fundamental mechanism for magmatic differentiation. In situ segregation of a strongly fractionated magma is commonly observed in shallow intrusions and lava flows in various scales (Greenough and Dostal, 1992; Carman, 1994; Goto, 1996; Philpotts et al., 1996; Caroff et al., 1997). Vein type segregation (Carman, 1994) is commonly

observed and many previous workers emphasized the importance of fracturing in incompletely solidifying magma for the segregation of interstitial melt (Wickham, 1987; Rutter and Neumann, 1995). Melt segregation by fracturing in incompletely crystallized magma is reported not only in mafic intrusions but also in granitic intrusions (Hibbard and Watters, 1985; John and Stünitz, 1997), and therefore, this process is one of the principle mechanisms of melt segregation during the crystallization of an intrusive body. Nevertheless, there is little discussion regarding the mechanical aspects of the formation of fractures and segregation of interstitial melt.

E-mail address: geshi@eri.u-tokyo.ac.jp (N. Geshi).

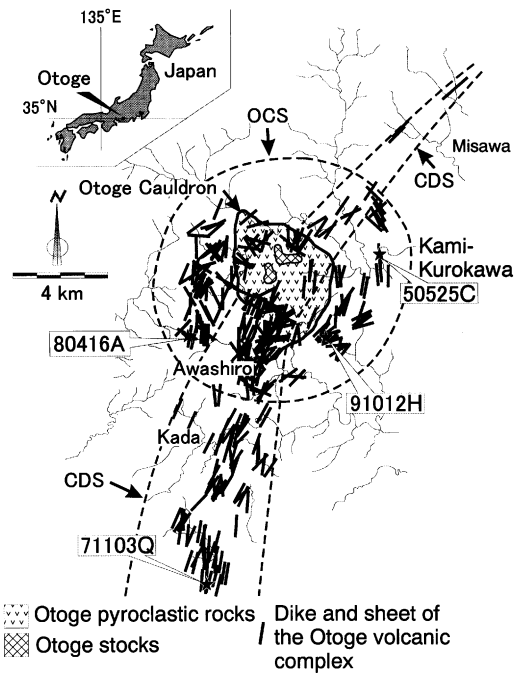


Fig. 1. Distribution of dikes and sheets of the Otoge volcanic complex. They were subdivided into the Otoge cone sheets and the Shitara central dike swarm by Takada (1987). Locations of samples for detailed studies are also shown by stars. Broken lines show the distribution areas of the Otoge cone sheets (OCS) and the Shitara central dike swarm (CDS).

In this paper, the author describes the structure, chemistry, and mineralogy of segregation veins in the Miocene Otoge volcanic complex, which mainly consists of mafic intrusive rocks. Most veins are filled with trachyandesite–trachyte, and their structural and compositional characters suggest in situ differentiation of the basaltic magma. The formation mechanism of trachyte veins and its implication in melt separation from a crystal mush will be discussed.

2. Geological background

The Otoge volcanic complex consists of cauldron-filling pyroclastic rocks and dike and sheet complexes, which are subdivided into Kamoyamagawa trachyte dikes, Otoge cone sheets, Shitara central dike swarm, and Otoge stocks (Takada, 1987, 1988; Geshi, 2000). They intruded into gneiss and granite of the Cretaceous Ryoke metamorphic

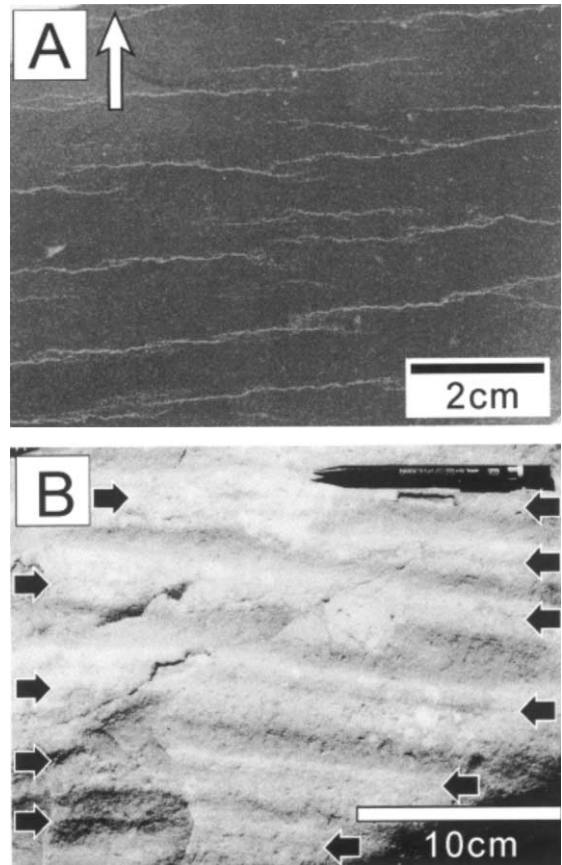


Fig. 2. Structures of trachyte veins. (A) Rhythmic development of trachyte veins consisting of a series of veinlets with echelon alignment in a 2 m thick aphyric trachytic andesite sheet. The cutting plane is vertical to the veins and parallel to the direction of shear suggested by the echelon alignment of the veinlets. An arrow indicates the direction of dike wall (0.5 m away). Sheet 50525C of the Otoge cone sheets. (B) Trachyte veins within pale bands. Arrows indicate trachyte veins. Weathered surface of an unrooted block from the dike 71103Q of the Shitara central dike swarm.

belt, sedimentary rocks of the Tertiary Shitara group, and volcanic rocks of the Shitara igneous complex during their latest stage of the igneous activity. The dikes and sheets were intruded at depths of 500–1000 m judging from the stratigraphy of the country rock. A K–Ar age of about 15 Ma was reported from one of the dikes of the Shitara central dike swarm by Tsunakawa et al. (1983).

The dikes and sheets with trachyte veins were formed at the last igneous stage of the Otoge igneous complex, and are divided into the Otoge cone sheets

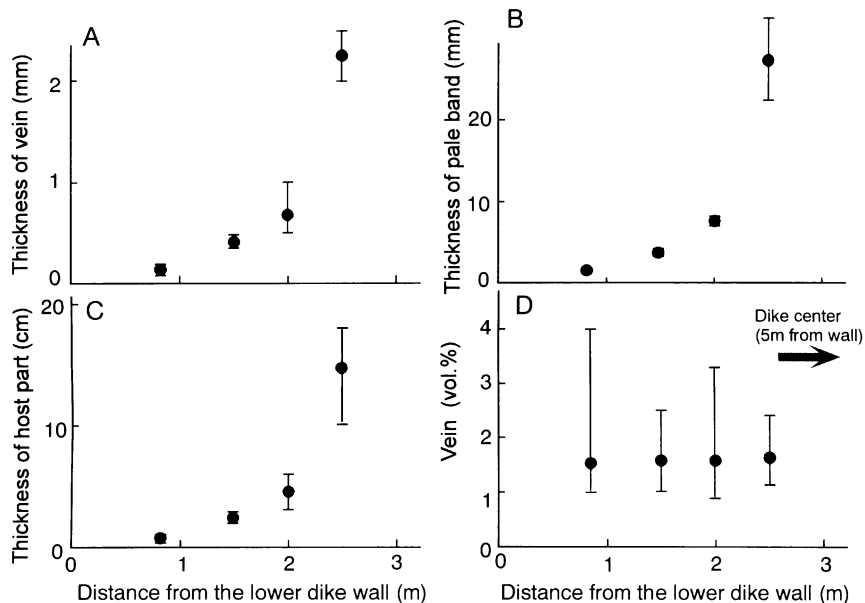


Fig. 3. Thickness of (A) veins, (B) pale band, and (C) host part plotted against the distance from the lower dike wall in a 10 m thick dike (91012H). (D) Volume percentage of the veins plotted against the whole-rock (host + pale band + vein). Bars indicate the variation range of data.

and the Shitara central dike swarm (Takada, 1987, 1988; Geshi, 2000). The Otoge cone sheets form a concentric sheet swarm dipping toward the center of the Otoge cauldron. The Shitara central dike swarm is a parallel and vertical dike swarm with a weak radial pattern (Fig. 1). Thickness of dikes and sheets ranges from less than one meter to several meters. Columnar joints perpendicular to the intrusion surface developed in some of the dikes and sheets.

The dikes and sheets consist of basalt–andesite with a very small amount of phenocrysts (usually less than 1 vol.%) of plagioclase, augite, olivine (\pm), and Fe–Ti oxides. The groundmass is holocrystalline except for in the chilled margin, which is several cm thick along the dike wall and consists of plagioclase laths up to 0.5 mm long, olivine, augite, Fe–Ti oxides up to 0.3 mm, and interstitial alkali-feldspar. The inner portion of dikes and sheets with trachyte veins contain a very small percentage of vesicles.

3. Structure and petrography of trachyte veins

The trachyte veins are several mm wide and occur

in alkaline basalt–trachyandesite dikes and sheets of the Otoge volcanic complex. In this paper, an intrusion containing trachyte veins is called a ‘host intrusion’, and the rock in which the veins occur is called ‘host part’. Trachyte veins are observed in most dikes and sheets having thickness greater than 1 m.

Trachyte veins develop anywhere inside a host intrusion except for the glassy chilled margins which are typically 0.5–1 cm thick. A series of trachyte vein consists of a complex of echelon-aligned veinlets connected to each other (Fig. 2A). The veinlets show oblique (10–30°) alignment against the direction of the series of veins. Individual veinlets are several mm to cm in length, and their thickness ranges from less than 1 mm to 1 cm. The basalt on either side of most trachyte veins exhibits slightly pale color with several mm to a cm width on weathered surface (pale band; Fig. 2B). Columnar joints perpendicular to dike walls sometimes develop and they clearly cut the trachyte veins.

In a marginal part of a host intrusion, a series of trachyte veins aligns parallel to the contact, and the thickness and spacing increase inward the host intrusion. In Fig. 3, variations of the thickness of veins,

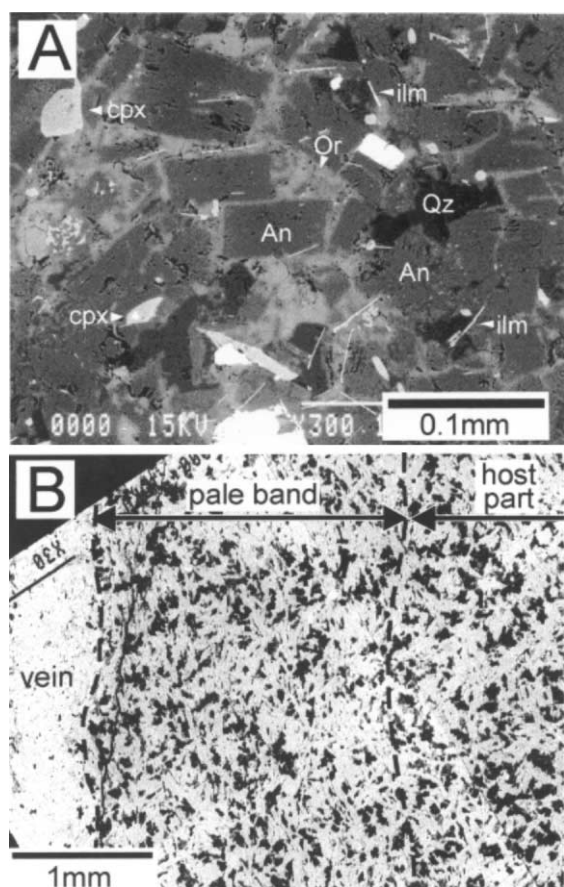


Fig. 4. Photomicrographs of a thin section of a trachyte vein (Sample 71103Q). (A) Anorthoclase (An), quartz (Qz), orthoclase (Or), clinopyroxene (cpx), and ilmenite (ilm) in a trachyte vein. Backscattered electron image. (B) Preferred orientation of plagioclase laths in the pale band along a trachyte vein. Backscattered electron image (negative image). Lighter colored parts are plagioclase and alkali-feldspars, and darker parts are olivine, clinopyroxene, and oxides.

pale bands, and their host parts are plotted against the distance from the wall for a dike (91012H), of which margin shows rhythmic development of veins. The sheet is about 10 m thick and consists of trachytic andesite. The rhythmic trachyte veins develop typically in the marginal part from 0.5 to 3 m from both the dike walls, and the thickness of the veins, pale bands, and their host part increases toward the center. The veins occupy about 1.5 vol.% of the whole-rock and the value is independent of the distance from the dike wall (Fig. 3D).

The trachyte veins consist of subhedral anortho-

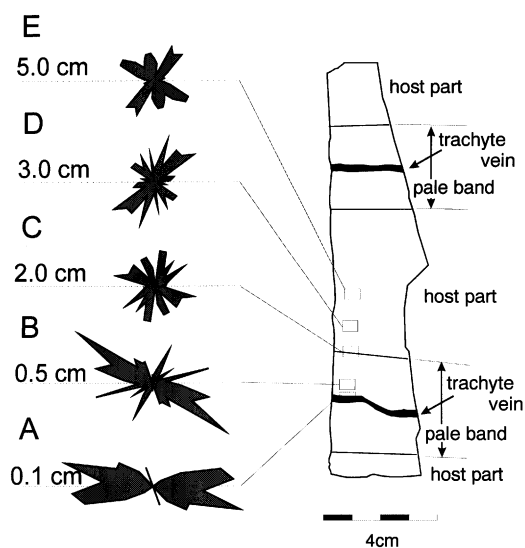


Fig. 5. The orientation diagrams of plagioclase fabric around trachyte veins in sample 80416A. Each analyzed area is about 8 mm² on a thin section perpendicular to the trachyte veins.

clase (An), clinopyroxene, and ilmenite with interstitial orthoclase and quartz (Fig. 4A). The size of An crystals varies from several tens to several hundreds μm . Clinopyroxene grains are elongated with length up to 100 μm . Ilmenite occurs as very thin tabular plates less than 10 μm thick. Some An and clinopyroxene have skeletal shapes. The modal composition of the trachyte veins is 60–65% alkali-feldspar, 5–10% clinopyroxene, several% ilmenite, and 15–25% interstitial orthoclase, quartz, and secondary clay minerals. No significant preferred orientation of minerals is recognized in the trachyte veins. The host part is holocrystalline alkali-basalt to trachyandesite, which consists of euhedral plagioclase, augite, and Fe–Ti oxides. Modal composition of the groundmass of the host part is about 55–65% plagioclase, 25–35% augite, several% magnetite, and several% interstitial alkali-feldspar, ilmenite, and quartz. Mineral assemblage and grain size in this ‘pale band’ are similar to those in the host part, but the pale band is more silicic as discussed in the next section.

Plagioclase crystals in the pale bands show a strong preferred orientation subparallel to the trachyte vein, whereas no remarkable preferred orientation is recognized outside the pale bands (Fig. 4B). Fig. 5 shows the orientation of plagioclase crystals in and around a

Table 1
Representative whole-rock compositions of the trachyte vein and their host part of dike 91012H

	CM ^a	Host	Vein1	Vein2
SiO ₂	56.4	53.2	67.9	69.4
TiO ₂	1.7	2.2	0.4	0.1
Al ₂ O ₃	15.5	15.3	16.4	16.0
FeO	8.4	9.7	2.4	2.9
MnO	0.2	0.2	0.1	0.0
MgO	2.4	3.0	0.4	0.5
CaO	4.7	6.6	0.8	0.9
Na ₂ O	5.3	5.1	5.8	6.1
K ₂ O	2.2	1.5	5.7	3.9
P ₂ O ₅	0.4	0.4	n.d. ^b	n.d. ^b
Total	97.1	97.0	99.9	99.9

^a CM: chilled margin of the dike.

^b n.d.: not determined.

pale band in the sample 80416A collected from a 4 m thick alkali-basalt sheet (locality shown in Fig. 1). Each vein in this sample is accompanied by a pale band approximately 4 cm thick. A preferred orientation subparallel to the vein is observed in the pale band (areas A and B), whereas no significant alignment occurs in the darker-colored part of the host part (areas C, D, and E).

Groundmass crystals along the trachyte veins are generally not truncated and show euhedral shapes against the vein. Phenocrysts in the host part stick

out to the trachyte vein and some isolated crystals and crystal clots derived from the host part are dispersed in the trachyte vein. The tip of a vein grades imperceptibly into the interstitial space of the host part and no crack is observed on the extension of the vein. The trachyte veins have no chilled margin against the host rock.

4. Whole-rock and mineral compositions

4.1. Analytical method

Whole-rock compositions of the host part and chilled margin were determined with an X-ray fluorescence analyzer (PHILIPS PW-1480) of the Geological Institute, the University of Tokyo. The analytical procedure was the same as that described by Yoshida and Takahashi (1997). Whole-rock compositions of trachyte veins and mineral compositions of plagioclase, clinopyroxene, olivine, and oxides were determined with an electron microprobe analyzer (EPMA; JEOL JCMS 733 Mk-II) of the Geological Institute, the University of Tokyo. Analytical procedures were the same as those described by Nakamura and Kushiro (1970) with the correction procedure of Bence and Albee (1968). Whole-rock compositions of trachyte veins were obtained by averaging the 200–400 analysis with a broad beam (25 μm in diameter) of each

Table 2
Representative mineral compositions of the trachyte vein and host part of sample 80417A

	Feldspar								Clinopyroxene							
	Trachyte vein				Host part (groundmass)				Trachyte vein				Host part (groundmass)			
	TV fel.1		TV fel.2		GPL1		GPL2		TCPX1		TCPX2		GCPX1		GCPX2	
	core	rim	core	rim	core	rim	core	rim	core	core	core	core	core	rim	core	rim
SiO ₂	66.0	67.3	65.2	67.3	55.6	67.2	55.2	67.5	SiO ₂	49.7	49.5	49.5	49.7	50.2	50.8	
TiO ₂	0.1	0.0	0.1	0.1	0.1	0.0	0.1	0.1	TiO ₂	1.2	1.3	1.8	1.6	1.2	0.6	
Al ₂ O ₃	20.5	19.2	21.4	18.7	27.4	19.7	27.7	19.0	Al ₂ O ₃	1.3	1.5	3.4	3.4	1.9	0.8	
FeO	0.6	0.6	0.6	0.7	0.7	0.7	0.6	0.5	FeO	20.2	20.3	10.5	10.9	12.7	16.5	
MnO	0.0	0.0	0.0	0.0	0.0	0.0	0.0	0.0	MnO	0.7	0.5	0.2	0.3	0.4	0.6	
MgO	0.0	0.0	0.0	0.0	0.1	0.0	0.1	0.0	MgO	7.6	7.3	14.1	13.5	13.5	11.9	
CaO	1.9	0.8	2.7	0.3	10.4	0.9	10.9	0.5	CaO	18.6	18.9	19.9	20.1	19.6	18.3	
Na ₂ O	9.1	8.0	8.7	7.9	5.3	8.7	5.0	7.8	Na ₂ O	0.5	0.6	0.4	0.4	0.4	0.3	
K ₂ O	1.8	3.9	1.4	5.0	0.2	2.8	0.2	4.6	K ₂ O	0.1	0.0	0.0	0.0	0.0	0.0	
An	10.4	4.9	14.5	2.4	52.0	5.3	54.6	3.2	Mg#	0.40	0.39	0.71	0.69	0.65	0.56	

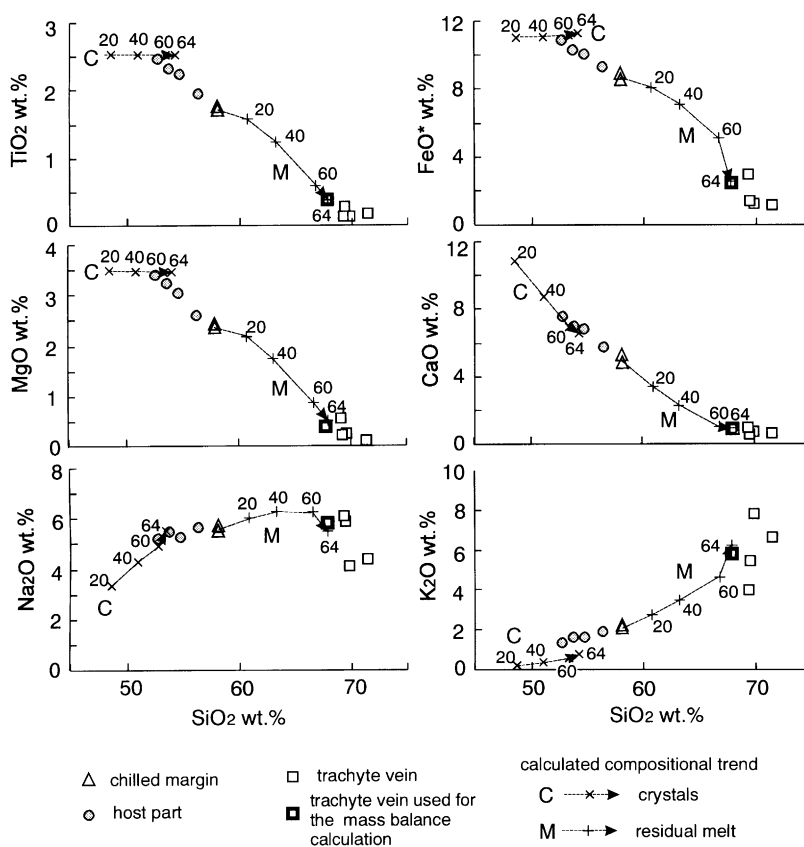


Fig. 6. Whole-rock compositions of trachyte veins, host parts, and the chilled margin of a sheet (91012H) plotted against the SiO₂ content. Whole-rock composition of veins are averaged values of 200–400 analyses by EPMA for each vein, and that of the host parts and chilled margin with XRF. Dashed lines show the compositional trends, which was calculated by MELTS program, of crystals (C) and residual melt (M) during fractional crystallization of the magma of the chilled margin to 64% of crystallinity. Numbers show the parentage of crystallinity.

sample. Raw analytical data for the whole-rock compositions were recalculated to 100 wt.%. Many dikes have undergone various degree of hydrothermal alteration in the studied area and they are partly or completely replaced by chlorite, sericite, calcite, and quartz. To minimize the effect of hydrothermal alteration, the least altered samples were selected with the procedure described in Geshi (2000). The selected samples for whole-rock analysis contain less than 5 vol.% of secondary minerals, and the effect of alteration is limited within 4% of the original values for the Na₂O and K₂O contents, and within 2% for the other oxides (Geshi, 2000). Representative compositions are listed in Table 1 (whole-rock) and Table 2 (minerals).

4.2. Whole-rock compositions

Fig. 6 shows the compositional variations of the trachyte veins and host part of a sheet (91012H). This dike is one of the Otoge cone sheets with thickness about 10 m and dipping about 40° toward the northwest, and consisting of aphyric basaltic andesite. The compositions of the chilled margin of the sheet are also shown in Fig. 6. Compositions of trachyte vein, host part, and chilled margin show a linear trend except for Na₂O and K₂O. Trachyte veins have higher contents of SiO₂ and K₂O and lower contents of TiO₂, FeO, MgO, and CaO than the chilled margin. The Na₂O contents of the veins show negative correlation and the K₂O shows positive correlation with the

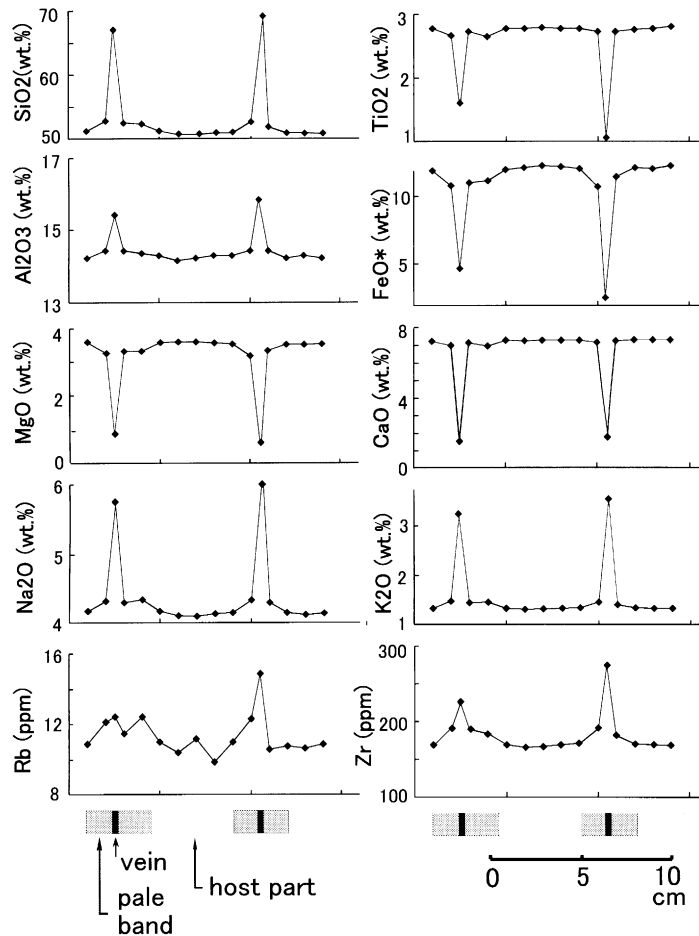


Fig. 7. Compositional profiles across trachyte veins of sample 80417A. The host intrusion is about 4.5 m thick and consists of phenocryst-poor alkali-basalt. Each analysis except for the trachyte veins are for a slab about 4 mm thick parallel to the trachyte vein.

SiO₂ content. The TiO₂, FeO, MgO, and CaO contents of the host parts show negative correlations and the Na₂O and K₂O contents show positive correlations with the SiO₂ content.

Fig. 7 shows the compositional profiles across trachyte veins with pale bands in the sample 80417A. Each point represents an averaged whole-rock composition of a slab about 4 mm thick parallel to the trachyte veins. The trachyte veins have higher concentrations of SiO₂, Na₂O, K₂O, Rb, and Zr and lower concentrations of TiO₂, FeO, MgO, and CaO than the host part. The pale bands have slightly higher concentrations of SiO₂, Na₂O, K₂O, Rb, and Zr and lower TiO₂, FeO, MgO, and CaO than the host part.

4.3. Mineral composition

4.3.1. Feldspar

The host part has plagioclase crystals with relatively high An content. The variation among the crystals within one sample is generally less than 20 in An content and the average An content correlates with their whole-rock composition. Fig. 8A shows the compositions of feldspars in a trachyte vein and the groundmass of the host part in a representative sample 80417A, one of the most primitive sheets in the Otoge igneous complex. The compositional variation of plagioclase in the host part ranges from 40 to 57 of the An content in their core, and they show strong normal zoning particularly at the rim. The

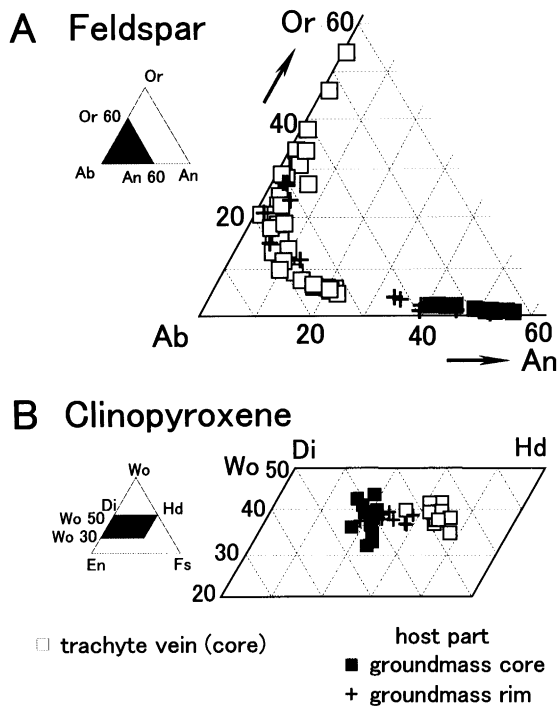


Fig. 8. Compositional variations of (A) feldspars and (B) clinopyroxenes in the trachyte veins and the host rock in the sample 80416A. Rim compositions of the crystals in the trachyte vein are difficult to determine because of alteration.

composition of the outermost rim is similar to feldspar in the trachyte vein. Subhedral An in the trachyte veins has 10–50 of the orthoclase content. The variation is owing to steep normal zoning particularly at the rim.

4.3.2. Clinopyroxene

The host part has clinopyroxene crystals with relatively high Mg# [$\text{Mg}/(\text{Mg} + \text{Fe})$]. Compositional variation among the clinopyroxene crystals within one sample is generally less than 0.2 in Mg# and they have good correlation with their whole-rock composition. The sheet 80417A has clinopyroxene phenocrysts ranging from 0.62 to 0.72 in Mg# (Fig. 8B). Clinopyroxene in the groundmass of the host part shows normal zoning with Mg# ranging from 0.72 to 0.54 from center to rim.

Clinopyroxenes in the trachyte veins show a larger compositional variation in Mg# than in their host part. The clinopyroxenes in the trachyte veins in the sample

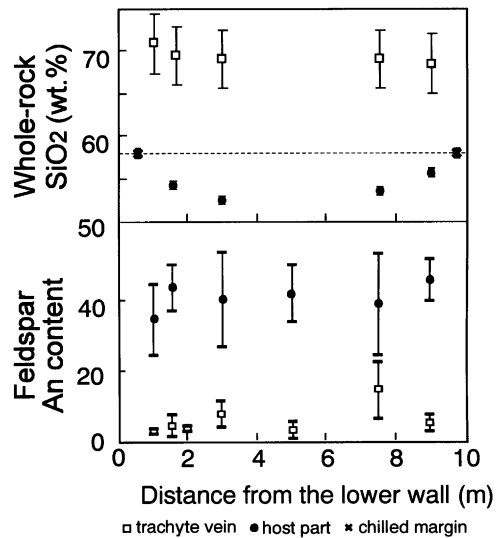


Fig. 9. Whole-rock SiO_2 contents and An contents of feldspars (core part of crystal) of the trachyte veins and their host rocks plotted against the distance from the lower dike wall (dike 91012H; about 10 m thick). The horizontal dashed-line indicates the whole-rock SiO_2 content of the chilled margin. Whole-rock compositions of the veins are averaged values of 200–400 analyses by EPMA for each vein. The plagioclase compositions are averaged values of 20–30 crystals for each vein. Vertical bars indicate the standard deviation for the averaged analysis.

80417A have Mg# ranging from 0.39 to 0.57 with most falling between 0.39 and 0.48. Compositional variation within a crystal is difficult to determine because of the small grain size.

4.4. Compositional variation within one dike

The whole-rock and mineral compositions of the trachyte veins are relatively constant in an intrusion. Fig. 9 shows the whole-rock SiO_2 content and An content of feldspar of veins and their host within the dike 91012H, of which whole-rock compositions of the veins, host parts, and chilled margin are shown in Fig. 6. The whole-rock SiO_2 content of the trachyte veins is about 70 wt.% and the An content of feldspar is about 5–10. These values are constant for the veins irrespective of the distance from the dike wall. The whole-rock SiO_2 content of the host part is lower than that of the chilled margin and decreases inward. It is about 54 wt.% at 1.5 m from the dike wall and about 52 wt.% at 3 m. The chilled margin contains about

Table 3
Comparison of observed and calculated compositions of the trachyte vein

Observed								Calculated at 64% crystallized	
Chilled margin	Trachyte vein	Host part	Mineral compositions of the host part				Residual melt	Crystals	
(9102H1)	(91012H5)	(91012H5)	Plagioclase	Olivine	Augite	Magnetite			
SiO ₂	58.4	67.9	56.5	63.5	36.6	51.8	0.2	67.8	54.1
TiO ₂	1.8	0.4	1.9	0.1	0.1	1.9	23.4	0.4	2.5
Al ₂ O ₃	16.0	16.4	15.9	22.7	0.1	1.4	0.3	16.7	15.7
FeO	8.7	2.4	9.3	0.3	37.6	14.0	76.0	2.4	11.6
MgO	2.4	0.4	2.6	0.0	24.9	12.6	0.0	0.5	3.3
CaO	4.9	0.8	5.7	4.5	0.6	18.7	0.0	1.0	6.6
Na ₂ O	5.5	5.8	5.6	8.0	0.0	0.3	0.0	5.5	5.5
K ₂ O	2.3	5.7	1.9	0.8	0.0	0.0	0.0	6.1	0.5
				(An 24)	(Mg# 0.54)	(Mg# 0.62)			
Modal composition		Observed	69	5	21	5			
		Calculated	75	3	17	6			

58 wt.% of SiO₂. The An content of feldspar of the host part is relatively constant (An_{25–50}) across the dike, which is higher than that of the veins.

5. Discussions

5.1. In situ separation of interstitial melt

The complete enclosure of the veins within a host intrusion, the systematic variation of veins within a host intrusion (Fig. 3), and the linear compositional relationship among the least fractionated veins, the host, and the chilled margin (Fig. 6) suggest the origin of trachyte veins by in situ separation of the interstitial melt during crystallization. The remarkable compositional zoning of the groundmass crystals in the host part shows in situ fractional crystallization of the host intrusion, which forms a residual melt with an evolved composition similar to trachyte veins. The nearly constant composition of veins and plagioclases in the host part within a dike (Fig. 9) suggests that a basaltic melt involved in the formation of the marginal part of the dikes has a constant bulk composition.

There is no clear evidence for an additional intrusion of trachytic magma into the host intrusions. First, the trachyte veins have no chilled texture at their margins, indicating that there was little if any thermal

contrast between the vein and the host intrusion when the trachyte veins were formed. Second, the veins are completely embedded in the host intrusion, and the thickness and interval of the veins systematically increase as the distance from the dike wall (Fig. 3). These facts negate the additional intrusion of the evolved magma, and are consistent with in situ segregation of residual melt in the host intrusion.

Last-squares calculation for the in situ fractional crystallization was performed based on the method of Bryan et al. (1969) to estimate the crystallinity at which melt separated. The fractionation of melt with the composition of the chilled margin was used to fit the composition of the vein of the dike 91012H with lowest SiO₂ content (68 wt.%; Fig. 6). The average compositions of plagioclase, olivine, clinopyroxene, and magnetite in the groundmass of the host part were used to represent composition of the crystallized phases (Table 3). The calculated composition of the residual melt matches closely the composition of the least differentiated trachyte vein when the original magma is crystallized approximately 64 vol.% (Table 3, Fig. 6). The obtained fraction of the minerals at 64 vol.% of crystallinity is 75 vol.% plagioclase, 3 vol.% olivine, 17 vol.% augite, and 6 vol.% magnetite, and the result is in good agreement with the actual modal ratio of the minerals in the host part (Table 3).

Fractionation trends of the residual melt and the crystals calculated by the MELTS program (Ghiorso

and Sack, 1995) are also shown in Fig. 6. The composition of the chilled margin of the dike 91012H was used as the initial magma composition, and the calculation was performed assuming fractional crystallization. It is assumed that the magma crystallized at 100 bar and oxygen fugacity -3 log units lower than FMQ with 0.1 wt.% of initial water content. These conditions are inferred from the stratigraphy of the host rocks, and the strongly reductive character and minor hydrous phases of the Otoge igneous complex (Geshi, 2000). The calculated melt composition at 64% crystallization by MELTS is very close to the least fractionated trachyte vein (Fig. 6). The depletion of Na_2O and enrichment of K_2O in the trachyte veins compared to the calculated melt composition (Fig. 6) can be explained by fractionation of sodic plagioclase ($\sim\text{An}_{10}$) after segregation of residual melt.

The variation of the whole-rock compositions of the host part, which is linear in the variation diagrams (Fig. 6), is interpreted to reflect the difference in the degree of melt extraction if the composition of the supplied basaltic magma was homogeneous and constant. This assumption is supported by the constant compositions of veins and plagioclase in the host parts (Fig. 9). The degree of melt extraction was larger in the inner part of the intrusion than in the marginal part judging from the profile of the SiO_2 contents of the host parts across an intrusion (Fig. 9).

5.2. Shear deformation, fracturing and segregation of interstitial melt

The preferred orientation of the groundmass crystals in the pale bands (Figs. 4B and 5), and the echelon arrangement of veinlets in a series of trachyte vein (Fig. 2A) show shearing in an incompletely solidified magma. It is argued that crystals in magma interconnect to construct a framework and that the magma behaves as a brittle material as soon as crystallinity

reaches a critical level (25–55%; Barth et al., 1994). The crystallinity beginning to form such a loose framework corresponds to the rigid percolation threshold (RPT) of Vigneresse et al. (1996), above which the framework can sustain stress despite the interstitial liquid still can flow through the framework.

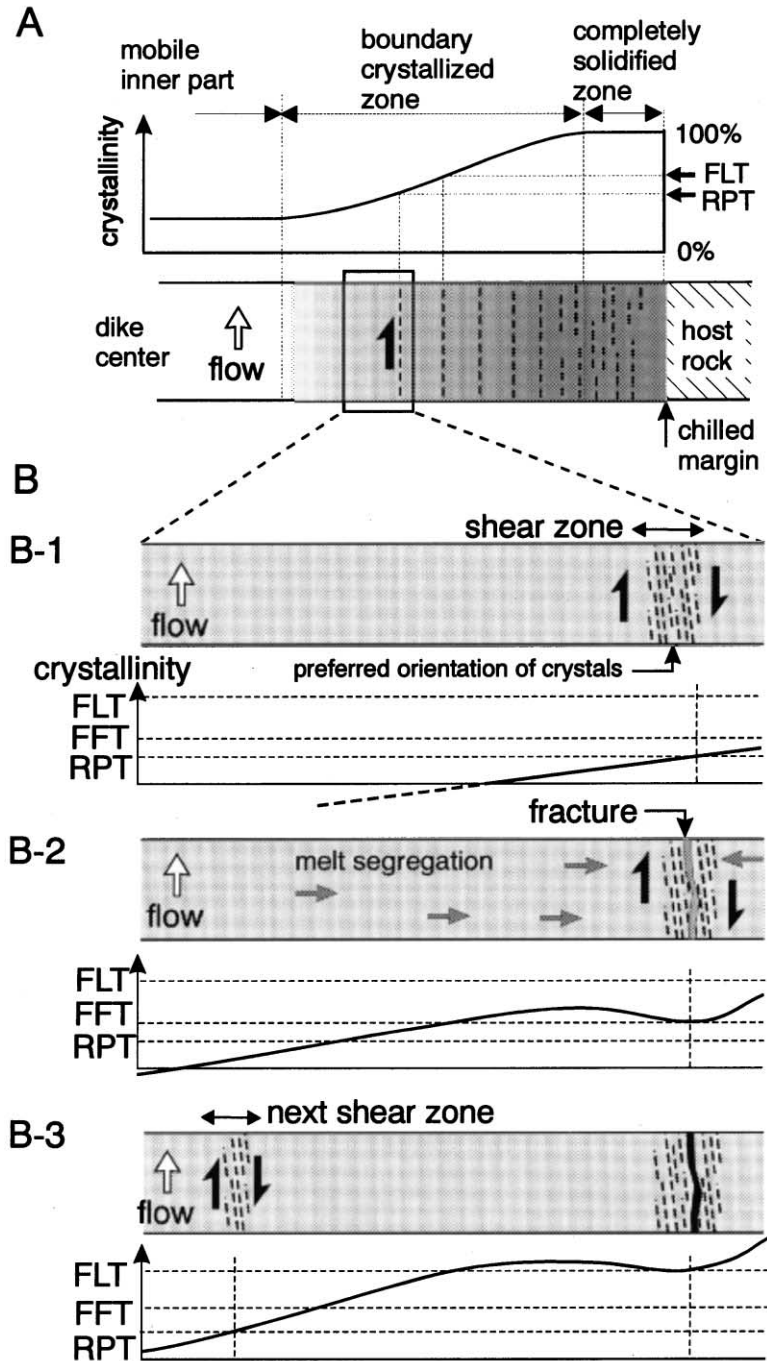
The crystallinity to form a framework depends on mineral assemblage and shape of crystals. Platy particles can form a highly porous aggregate by interconnection of grains at a low solid fraction (Burgers, 1938; Philpotts et al., 1998), whereas a granular framework of spherical grains will be formed at around two-third of solid fraction (Vigneresse et al., 1996). A framework of olivine crystals with rounded shape will form the ‘granular framework’ with a high solid fraction. Measurements in drill holes in Hawaiian lava lakes show that the crystallinity at the bottom of a rigid crust, which mainly consists of olivine crystals, was 55% at Makaopuhi (Wright and Okamura, 1977) and 65% at Kilauea Iki (Helz, 1980), and these values coincide with the model of granular framework. On the other hand, platy plagioclases can form a highly porous aggregate. Melting experiments on tholeiitic basalt showed the formation of a crystal framework of plagioclase around 30% crystallinity (Philpotts et al., 1998). Holyoke flood-basalt flow is estimated to have a brittle framework of plagioclase crystals at 33% crystallinity (Philpotts et al., 1996).

Plagioclase is the dominant phase in the groundmass (Table 3) and the modeling of crystallization with MELTS calculation shows that the plagioclase is the first liquidus phase for the chilled margin composition. The preferred orientation of plagioclase around the trachyte veins (Fig. 5) suggests rotation of plagioclase crystals in a dense crystal mush. Based on the experimental study by Philpotts et al. (1996), the basaltic magma in the Otoge igneous complex is inferred to have behaved as a brittle substance at around 30% of crystallinity with the framework of plagioclases.

Fig. 10. Schematic illustration of the formation of trachyte veins (dashed line). (A) Outline of the conditions. A dike is cooling and crystallizing from the walls, but still the inner portion is moving. Crystallinity increases toward the dike wall. (B) Development of vein formation. B-1: Shear stress in the boundary layer is localized at the front of RPT parallel to the isotherm. A preferred orientation of plagioclase crystals is formed by shear deformation. B-2: The stress in the boundary layer is consumed by the deformation in the localized shear zone. Crystallinity of the shear zone reaches the fracture formation threshold (FFT), and a series of fractures is formed. Interstitial melt segregates into the shear zone by dilatancy of the shear zone and dilation of a fracture. B-3: When the crystallinity of shear zone reaches the FLT, dilation of the fracture is prevented and the localization of the shear jump to the front of the RPT and a new shear zone is created.

Compositional relationship among the trachyte vein, host part, and chilled margin shows, however, that the melt segregation occurred at around 65% of crystallization (Table 3, Fig. 6), and this value is much

higher than the crystallization expected from the above model. A possible explanation for the difference in the crystallinity is that the small value (~30 vol.%) is for the formation of crystal framework



and the large one (~60 vol.%) is for the fracturing of the mush. A newly formed crystal framework at the low crystallinity (~30 vol.%) is so fragile that it is not capable of developing a continuous fracture. Shear deformation in the crystal mush at low crystallinity will cause local disruption of the bond of crystals in framework, and individual crystals rotate to form a preferred orientation. Continuous fracturing of the crystal framework will occur at higher crystallinity (~60 vol.%), at which the rotation of individual crystal is prevented by the rigid connection of crystals. The preferred orientation observed in the pale band (Figs. 4B and 5) may be the result of the rotation of platy crystals in the crystal mush with low-crystallinity. The trachyte veins which cut the preferred orientation of the pale band suggest that the fracturing occurred after the formation of the preferred orientation. From these considerations, the following sequence of events after reaching RPT is proposed. With progress of crystallization, the framework becomes more rigid, and shearing in the crystal mush will cause tearing of the framework and form a series of dilation fractures (fracture forming threshold; FFT). Interstitial melt will be drawn to the dilation fracture by pressure gradient and form a segregation vein. Finally, growth of the fracture will be prevented by the decrease of melt fraction due to cooling (fracture locked threshold; FLT).

The subparallel development of a series of trachyte veins and the echelon alignment of veinlets in a series of veins indicate that a series of trachyte veins is a shear zone formed by the viscous drag of molten inner part (Shelley, 1985; Smith et al., 1993). The veinlets are oblique to that of a series of veins with about 20° and show echelon alignment (Fig. 2A). This suggests that the veinlets are Riedel shear-crack formed by localized shearing. Continuous deformation caused the interconnection of the veinlets and formed a series of trachyte vein subparallel to the dike wall. Sheared structures formed by magmatic flow recorded in dike margins are commonly observed (Shelley, 1985; Philpotts and Asher, 1994; Geshi, 2000), and the echelon-aligned trachyte veins is one of the shear structures in the crystallizing magma.

The parallel development of echelon-aligned veins and the lack of conjugate pair suggest that the role of magmatic pressure flattening (Smith et al., 1993) is small for the formation of trachyte veins. The role of

the gravitational instability of residual melt was also slight excepting the central zone because the trachyte veins are observed in the marginal part of intrusions irrespective of the form of the host intrusions (sill or dike) and the veins develop both near the roof and floor of sills.

The rhythmic development of the series of trachyte veins parallel to the dike walls and the increasing spacing toward the dike center show that the position of localization of shear was controlled by successive cooling from the dike wall. A schematic model for the formation of trachyte veins is shown in Fig. 10. The crystallinity of magma increase outward in the boundary crystallized zone (Fig. 10A). Shear in the boundary-crystallized layer will be localized around the front of RPT (Fig. 10B-1). Interstitial melt will be drawn toward the shear zone according to the gradient of fluid pressure caused by dilatancy of the shear zone (Emmons, 1940; Marsh, 1981; Smith, 1997; Claudio and Handy, 2000). As a result, the melt fraction in the shear zone becomes higher than the neighborhood. Segregation of melt to the shear zone accelerates the localization of the shear because the deformation will localize to the mechanically weakest part and the rigidity of the crystal mush depends on its melt fraction, and the continuous shear zone subparallel to the shear is formed (Claudio and Handy, 2000). Once a shear zone is formed in a deformed zone, the deformation of the boundary layer is concentrated in the generated shear zone. Successive deformation causes tearing of the crystal mush in the shear zone at the FFT, and the generated fracture draws interstitial melt from the surrounding crystal mush (Fig. 10B-2). Successive cooling increases the crystallinity of the deforming zone and it prevents the growth of the fractures at the FLT. When dilation of the fracture is prevented, stress in the boundary layer can no more be consumed in the existing shear zone and a new shear zone is formed at the front of RPT (Fig. 10B-3). In this manner, trachyte veins were formed periodically in the marginal part of an intrusion during continuous cooling of the intrusion.

The randomly developed trachyte veins in the central portion of the intrusion was formed by another mechanism such as buoyant instability of the residual melt. Magma could not flow when solidification reached the central part of the intrusion and the orientation of the veins was less controlled by the shear.

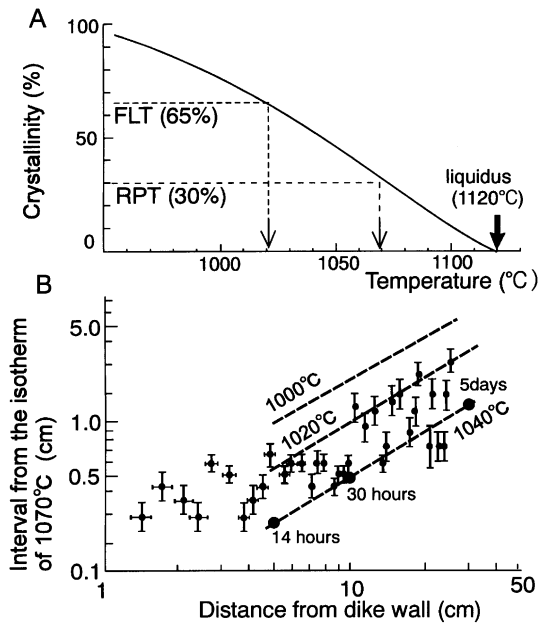


Fig. 11. (A) The crystallinity of the magma (50525C) during cooling at 100 bar and 0.1 wt.% of water content calculated by MELTS. Temperature for RPT and FLT corresponds to 1070 and 1020°C, respectively. (B) Intervals of 1000, 1020, and 1040°C isotherms from 1070°C isotherm as a function of distance from the dike wall in a cooling dike 2 m thick, compared with the observed interval of trachyte veins in a sheet about 2 m thick (50525C). Bars of each point indicate the variations of the interval of veins and the distance from the dike wall.

The continuous trachyte vein in the central part was the melt channel through which the buoyant residual melt was transported upward, although there is no significant evidence for the separation of residual melt in the intrusions of the Otoge volcanic complex exposed at the present erosion level.

5.3. Spacing of trachyte vein

The interval of trachyte veins in the present model corresponds to the time difference of the two isotherms of RPT (Vignerresse et al., 1996), at which shear deformation localizes in a loose framework of crystals, and FLT, at which dilation of a crack is prevented (Fig. 10B). As cooling proceeds, the thermal gradient in the marginal portion of a dike becomes smaller and the interval of the two isotherms increases. As a result, the spacing of trachyte veins increases inward.

To examine this model quantitatively, crystallization

of magma and temperature development of a dike with 2 m thick (50525C dike in Fig. 3) was calculated numerically. A crucial assumption made here is that RPT and FLT are only dependent on temperature, which implies that the shear stress was held constant during the solidification of the marginal part of the dike with rhythmic development of the trachyte veins. The crystallinity of the magma with the composition of chilled margin of the dike 50525C at a given temperature was calculated with MELTS program. The initial temperature of the magma is assumed to be the liquidus temperature (1120°C), because the minor phenocrysts suggest that the temperature of magma is at its liquidus. Initial temperature of the host rock is assumed to be 100°C, because the effect of hydrothermal alteration is slight in the host rock (Geshi, 2000). The magma is assumed to have cooled from the dike wall only by heat conduction through the magma in the dike. Thermal diffusivity of the crystallizing magma and the host rock is taken as $8 \times 10^{-7} \text{ m}^2 \text{ s}^{-1}$, specific heat of the magma and host rock $1.3 \text{ J g}^{-1} \text{ K}^{-1}$, and latent heat of crystallization 300 J g^{-1} after Huppert and Sparks (1988). The crystallinity of the magma was obtained as a function of the temperature (Fig. 11A). The crystallinity of the magma reaches 30% (RPT) at 1070°C (Fig. 11A). Although it is difficult to determine the crystallinity of FFT because of the uncertainty of the behavior of crystal mush, the value should be smaller than 65% but greater than 30%. In this model, dilation of fracture was prevented at 65% of crystallinity (FLT) at 1020°C (Fig. 11A).

Fig. 11B shows the interval of these isotherms of 1000, 1020, and 1040°C from the isotherm of 1070°C (front of RPT, 30% of the magma crystallization). The isotherms move inward and the interval of the isotherms increases as the dike cools. The observed interval of the trachyte veins are plotted between the lines of 1020 and 1040°C. This thermal condition is lower than RPT but higher than FLT, and is consistent with the present model. The isotherm of 1040°C reaches 5 cm from the dike wall in $5 \times 10^4 \text{ s}$ (ca. 14 h) after the intrusion, 10 cm in $1 \times 10^5 \text{ s}$ (ca. 30 h), and 30 cm in $4 \times 10^5 \text{ s}$ (about 5 days).

5.4. Escape of residual melt through trachyte veins

The linear variation of the whole-rock compositions of the host parts (Fig. 6) shows that the host

parts are a mixture of the residual melt with the trachytic compositions and the crystals. The variation represents the difference in the melt fraction trapped in the host part. The compositions of the veins, pale band, and host part, and their volume fraction suggest that the host part 1 m from the wall (91012H5) contains 18 vol.% of residual melt with trachytic composition, which was formed at the 64% crystallinity. This shows that the residual melt was about 20 vol.% against the initial volume of the magma extracted from the host part. The volume fraction of the veins is, however, about 1 vol.% of the whole-rock (vein + pale band + host part), and this suggests that most of the trachytic melt which segregated in the veins escaped out of the observed rock. Systematic decrease of SiO₂ content of the host part (Fig. 9) shows that the degree of melt escape is larger in the inner part of the dike.

The density contrast between the residual melt with trachyte composition and the surrounding crystal mush drive the upward flow of segregated melt. Most of the trachyte melt may escape upward through trachyte vein, and accumulate around the upper tip of the dike, although the melt-accumulated part cannot be observed.

6. Comparison with other in situ differentiated intrusions

The common occurrence of segregation veins has been previously noticed in many shallow intrusions. Carman (1994) reviewed the occurrence of syenite bodies in many shallow intrusions and lava flows, and classified them by their structural characters. Trachyte veins in Otoge volcanic complex correspond to the plagioclase-poor syenite sheet (PP sheet) and stringers of Carman (1994). No other type of Carman (1994) was observed in this complex. Carman (1994) concluded that rifting of a rigid crystal framework and residual melt filtration after crystallization by about 50 wt.% of the parent magma formed the PP syenite sheets and stringers, and inferred that cooling contraction caused fracturing of the crystal framework. Goto (1996) reported rhythmic segregation veins with 'pale band' in a mushroom-shaped intrusion and concluded that cooling contraction caused the fractures parallel to the intrusion wall. A preferred orientation of the

groundmass crystals near the veins and local echelon alignment of the trachyte veinlets in the Otoge igneous complex suggests the importance of shear deformation and fracturing by the movement of magma, and their parallel development was controlled by the gradient of the rigidity of the crystal mush depending on their crystallinity.

Fracturing in highly crystallized magma is an effective mechanism to segregate residual melt with strongly fractionated composition, because crystals are locked in a crystal framework and only an interstitial melt drew into the fracture. Although a single fracture may segregate only a little liquid, repeated fracturing will accumulate larger amounts of melts. Veinlets with evolved composition associated with shear zones are observed in felsic plutons (Adamello massif; John and Stünitz, 1997) and in ocean floor gabbros (ODP 735B; Dick et al., 1991) in much larger scale, and these examples suggest that the deformation-assisted melt segregation is a common process in igneous bodies. The shear deformation discussed here is a general process in a crystallizing mobile magma body and is an important mechanism in the early stage of separation of the strongly-evolved residual melt.

7. Conclusions

Trachyte veins in the intrusive bodies of the Otoge volcanic complex were formed by in situ segregation of the residual melt during the late stage of crystallization of the host intrusion. Mass balance calculation shows that the residual melt with trachyte composition was formed at about 65% crystallization of the host magma.

A preferred orientation of the groundmass crystals near the veins and local echelon alignment of veinlets suggest localization of shear deformation and fracturing in a crystal mush. Dilation of cracks drew the interstitial liquid and formed trachyte veins. Flow in the central portion with lower crystallinity caused the localized shear deformation in the boundary-crystallized layer.

Cooling from the dike wall controlled the orientation and spacing of the fractures. Periodic localization of shear and fracturing thus took place successively to form oscillatory trachyte veins in the marginal portion of the intrusions.

Shear deformation and fracturing in highly crystallized magma is an effective mechanism to segregate residual melt with strongly fractionated composition, because crystals are locked in a crystal framework and only an interstitial melt drew into the fracture. Concentration of shear in the marginal part of a magma body is common phenomenon and the melt segregation by shear presented here should be the general process in a solidifying magma body.

Acknowledgements

I thank Hiroko Nagahara and Kazuhito Ozawa for valuable discussions and encouragement during this work. I also thank Akira Takada for his valuable suggestions and helpful information for the field survey. Hideto Yoshida is thanked for XRF and EPMA analysis, and helpful discussion during this work. Critical reviews by Anthony R. Philpotts and John V. Smith greatly improved the manuscript. I am also indebted to Susumu Ikeda, Hikaru Iwamori, Atsushi Toramaru, and Mitsuhiro Toriumi for their important advice. This work was supported by the Japanese Society for the Promotion of Science for Japan Junior Scientists.

References

- Barth, G.A., Kleinrock, M.C., Helz, R.T., 1994. The magma body at Kilauea Iki lava lake: potential insights into mid-ocean ridge magma chambers. *J. Geophys. Res.* 99, 7199–7217.
- Bence, A.E., Albee, A.L., 1968. Empirical correction factors for the electron microanalysis of silicates and oxides. *J. Geol.* 76, 382–403.
- Bryan, W.B., Finger, L.W., Chayes, F., 1969. Estimating proportions in petrographic mixing equations by least-squares approximation. *Science* 163, 926–927.
- Burgers, J.M., 1938. *Second Report on Viscosity and Plasticity*. Nordemann, New York, pp. 113–184.
- Carman Jr., M.F., 1994. Mechanisms of differentiation in shallow mafic alkaline intrusion, as illustrated in the Big Bend area, west Texas. *J. Volcanol. Geotherm. Res.* 61, 1–44.
- Caroff, M., Ambrics, C., Maury, R.C., Cotton, J., 1997. From alkali basalt to phonolite in hand-size samples: vapor-differentiation effects in the Bouzentes lava flow (Central, France). *J. Volcanol. Geotherm. Res.* 79, 47–61.
- Claudio, L.R., Handy, M.R., 2000. Syntectonic melt pathways during simple shearing of a partially molten rock analogue (Norcamphor-Benzamide). *J. Geophys. Res.* 105, 3135–3149.
- Dick, H.J.B., Meyer, P.S., Bloomer, S., Kirby, S., Stakes, D., Mawer, C., 1991. Lithostratigraphic evolution of an in situ section of oceanic layer 3. *Proc. ODP, Scientific Results* 118, 439–538.
- Emmons, R.C., 1940. The contribution of differential pressure to magmatic differentiation. *Am. J. Sci.* 238, 1–21.
- Geshi, N., 2000. Fractionation and magma mixing within intruding dike swarm: evidence from the Miocene Shitara-Otoge igneous complex, central Japan. *J. Volcanol. Geotherm. Res.* 98, 127–152.
- Ghiorsso, M.S., Sack, R.O., 1995. Chemical mass transfer in magmatic processes IV. A revised and internally consistent thermodynamic model for the interpolation and extrapolation of liquid-solid equilibria in magmatic systems at elevated temperatures and pressures. *Contrib. Mineral. Petrol.* 119, 197–212.
- Goto, Y., 1996. A rhythmically banded basaltic andesite intrusion in the Shiretoko Peninsula, Hokkaido, Japan. *J. Jpn. Min. Petrol. Econ. Geol.* 91, 427–442.
- Greenough, J.D., Dostal, J., 1992. Cooling history and differentiation of a thick North Mountain Basalt flow (Nova Scotia, Canada). *Bull. Volcanol.* 55, 63–73.
- Helz, R., 1980. Crystallization history of Kilauea Iki lava lake as seen in drill core recovered in 1967–1979. *Bull. Volcanol.* 43, 675–701.
- Hibbard, M.J., Watters, R.J., 1985. Fracturing and diking in incompletely crystallized granitic plutons. *Lithos* 18, 1–12.
- Huppert, H., Sparks, R.S.J., 1988. The generation of granitic magmas by intrusion of basalt into continental crust. *J. Petrol.* 29, 599–624.
- John, B.E., Stünitz, H., 1997. Magmatic fracturing and small-scale melt segregation during pluton emplacement: evidence from the adamello massif (Italy). In: Bouchez, et al. (Eds.), *Granite: From Segregation of Melt to Emplacement Fabrics*. Kluwer academic publishers, Dordrecht, pp. 55–74.
- Marsh, B.D., 1981. On the crystallinity, probability of occurrence, and rheology of lava and magma. *Contrib. Mineral. Petrol.* 78, 85–98.
- Nakamura, Y., Kushiro, I., 1970. Compositional relations of coexisting orthopyroxene, pigeonite and augite in a tholeiitic andesite from Hakone volcano. *Contrib. Mineral. Petrol.* 26, 265–275.
- Philpotts, A.R., Asher, P.M., 1994. Magmatic flow-direction indicators in a giant diabase feeder dike. *Conn. Geol.* 22, 363–366.
- Philpotts, A.R., Carroll, M., Hill, J.M., 1996. Crystal-mush compaction and the origin of pegmatitic segregation sheets in a thick flood-basalt flow in the Mesozoic Hartford basin. *Conn. J. Petrol.* 37, 811–836.
- Philpotts, A.R., Shi, Y., Brustman, C., 1998. Role of plagioclase crystal chains in the differentiation of partially crystallized basaltic magma. *Nature* 395, 343–346.
- Rutter, E.H., Neumann, D.H.K., 1995. Experimental deformation of partially molten westerly granite under fluid-absent conditions, with implications for the extraction of granitic magmas. *J. Geophys. Res.* 100, 15,697–15,715.
- Shelley, D., 1985. Determining paleo-flow directions from groundmass fabrics in the Lyttelton radial dykes, New Zealand. *J. Volcanol. Geotherm. Res.* 25, 69–79.
- Smith, J.V., Miyake, Y., Yamauchi, S., 1993. Flow direction and groundmass shear zones in dykes, Shimane Peninsula. *Jpn. Geol. Mag.* 130, 117–120.

- Smith, J.V., 1997. Shear thickening dilatancy in crystal-rich flows. *J. Volcanol. Geotherm. Res.* 79, 1–8.
- Takada, A., 1987. Structure of a cauldron in the Otoge ring complex, Shitara district, Aichi Prefecture, central Japan. *J. Geol. Soc. Jpn.* 93, 107–120 (in Japanese with English abstract).
- Takada, A., 1988. Subvolcanic structure of the central dike swarm associated with the ring complexes in the Shitara district, central Japan. *Bull. Volcanol.* 50, 106–118.
- Tsunakawa, H., Kobayashi, Y., Takada, A., 1983. K–Ar ages of dikes in Southwest Japan. *Geochem. J.* 17, 265–268.
- Vignerresse, J.L., Barbey, P., Cunet, M., 1996. Rheological transitions during partial melting and crystallization with application to felsic magma segregation and transfer. *J. Petrol.* 37, 1579–1600.
- Wickham, S.M., 1987. The segregation and emplacement of granitic magmas. *J. Geol. Soc. London* 144, 281–297.
- Wright, T.L., Okamura, R.T., 1977. Cooling and crystallization of tholeiitic basalt, 1965 Makaopuhi lava lake, Hawaii. USGS Prof. Paper 1004, 78 pp.
- Yoshida, H., Takahashi, N., 1997. Chemical behavior of major and trace elements in the Horoman mantle diapir, Hidaka belt, Hokkaido, Japan. *J. Jpn. Assoc. Min. Petrol. Econ. Geol.* 92, 391–409 (in Japanese with English abstract).